Monthly Notices of the ROYAL ASTRONOMICAL SOCIETY LETTERS

Mon. Not. R. Astron. Soc. **408,** L61–L65 (2010) doi:10.1111/j.1745-3933.2010.00928.x

The magnetic field and the evolution of element spots on the surface of the HgMn eclipsing binary AR Aur⋆

S. Hubrig,[1]† I. Savanov,[2] I. Ilyin,[1] J. F. González,[3] H. Korhonen,[4] H. Lehmann,[5] M. Schöller,[4] T. Granzer,[1] M. Weber,[1] K. G. Strassmeier,[1] M. Hartmann[5] and A. Tkachenko[5]

[1]*Astrophysikalisches Institut Potsdam, An der Sternwarte 16, 14482 Potsdam, Germany*
[2]*Institute of Astronomy, Russian Academy of Sciences, Pyatnitskaya 48, Moscow 119017, Russia*
[3]*Instituto de Ciencias Astronomicas, de la Tierra, y del Espacio (ICATE), 5400 San Juan, Argentina*
[4]*European Southern Observatory, Karl-Schwarzschild-Str. 2, 85748 Garching bei München, Germany*
[5]*Thüringer Landessternwarte, 07778 Tautenburg, Germany*

Accepted 2010 July 28. Received 2010 July 28; in original form 2010 June 25

ABSTRACT

The system AR Aur is a young late B-type double-lined eclipsing binary with a primary star of HgMn peculiarity. We applied the Doppler imaging method to reconstruct the distribution of Fe and Y over the surface of the primary using spectroscopic time series obtained in 2005 and from 2008 October to 2009 February. The results show a remarkable evolution of the element distribution and overabundances. Measurements of the magnetic field with the moment technique using several elements reveal the presence of a longitudinal magnetic field of the order of a few hundred gauss in both stellar components and a quadratic field of the order of 8 kG on the surface of the primary star.

Key words: stars: abundances – binaries: eclipsing – binaries: spectroscopic – stars: chemically peculiar – stars: individual: AR Aur – stars: magnetic field.

1 INTRODUCTION

The system AR Aur (HD 34364, B9V+B9.5V) with an orbital period of 4.13 d at an age of only 4×10^6 yr belongs to the Aur OB1 association. Since its primary star of HgMn peculiarity is exactly on the zero-age main sequence (ZAMS) while the secondary is still contracting towards the ZAMS, it presents the best case to study evolutionary aspects of the chemical peculiarity phenomenon. Variability of spectral lines associated with a large number of chemical elements was reported for the first time for the primary component of this eclipsing binary by Hubrig et al. (2006a). AR Aur belongs to the well-defined subclass of chemically peculiar HgMn stars of B7–B9 spectral types with $T_{\rm eff}$ between 10 000 and 14 000 K. These stars exhibit abundance anomalies of several elements, e.g. overabundances of Hg, Mn, Ga, Y, Cu, Be, P, Bi, Sr, Zr and deficiencies of He, Al, Zn, Ni and Co (e.g. Castelli & Hubrig 2004). The fundamental parameters of this system are already well known from careful studies carried out in the 1980s and 1990s (e.g. Nordström & Johansen 1994) and are summarized in our previous study (Hubrig et al. 2006a).

Variations in Hg and Y line profiles of AR Aur were first detected by Takeda, Takada & Kitamura (1979). Doppler maps for the elements Mn, Sr, Y and Hg using nine spectra of AR Aur observed at the European Southern Observatory with the UV-Visual Echelle Spectrograph (UVES) spectrograph at UT2 in 2005 were for the first time presented at the IAU Symposium 259 by Savanov et al. (2009). For AR Aur, standard Doppler imaging (DI) techniques can be applied after the spectrum of the secondary star is removed and the orbital radial velocity is subtracted. As we already reported in 2006, the secondary does not show line-profile variability and the luminosity ratio between the components is constant, allowing us to properly separate the spectra of the two components (e.g. González & Levato 2006). The study presented here was motivated by the results of the recently published work on spectroscopic time series of another HgMn star, HD 11753, which revealed noticeable temporal changes in the surface distribution of several elements, indicating a dynamical chemical spot evolution (Briquet et al. 2010). To prove the presence of a dynamical evolution of spots on the surface of AR Aur, we obtained new spectroscopic data and constructed a second map of the stellar surface via DI. To pinpoint the mechanism responsible for the surface structure formation in HgMn stars, we carried out spectropolarimetric observations of AR Aur and

⋆Based on observations obtained at the 2.56-m Nordic Optical Telescope on La Palma, the Karl-Schwarzschild-Observatorium in Tautenburg and the STELLA robotic telescope on Tenerife.

†E-mail: shubrig@aip.de

Table 1. Logbook of the spectroscopic observations of AR Aur. The HJD is given with respect to $HJD_0 = 2450\,000$.

HJD	Phase	S/N	Telescope	HJD	Phase	S/N	Telescope	HJD	Phase	S/N	Telescope
2516.7220	0.7068	140	SOFIN	4756.6637	0.4543	208	TLS	4817.6736	0.2106	179	STELLA
2518.7505	0.1974	130	SOFIN	4757.5512	0.6690	292	TLS	4818.4143	0.3897	154	STELLA
2588.5729	0.0845	173	SOFIN	4757.5728	0.6742	312	TLS	4818.6690	0.4513	162	STELLA
2588.6458	0.1021	129	SOFIN	4759.5940	0.1631	182	TLS	4819.4340	0.6364	164	STELLA
2589.6831	0.3530	117	SOFIN	4759.6156	0.1683	211	TLS	4820.3626	0.8610	114	STELLA
2590.6895	0.5964	211	SOFIN	4774.5775	0.7871	147	STELLA	4821.3568	0.1014	160	STELLA
2595.6398	0.7937	200	SOFIN	4775.5629	0.0254	138	STELLA	4822.4156	0.3575	150	STELLA
2596.6601	0.0404	257	SOFIN	4782.5702	0.7203	199	TLS	4822.6629	0.4173	158	STELLA
2599.6243	0.7574	211	SOFIN	4782.5919	0.7255	186	TLS	4841.2991	0.9248	329	TLS
2599.6341	0.7597	217	SOFIN	4783.4632	0.9362	139	STELLA	4841.3208	0.9301	338	TLS
2600.6964	0.0167	206	SOFIN	4808.4109	0.9702	198	STELLA	4842.5493	0.2272	287	TLS
2600.7082	0.0195	194	SOFIN	4808.6571	0.0298	159	STELLA	4842.5709	0.2324	251	TLS
2601.6524	0.2479	250	SOFIN	4809.4120	0.2124	156	STELLA	4843.3326	0.4167	274	TLS
2601.6631	0.2505	214	SOFIN	4809.7303	0.2894	168	STELLA	4843.3543	0.4219	289	TLS
2650.4973	0.0614	238	SOFIN	4811.6648	0.7573	185	STELLA	4875.4747	0.1907	168	TLS
2650.5291	0.0691	215	SOFIN	4812.4485	0.9468	157	STELLA	4875.5040	0.1978	167	TLS
4756.6421	0.4491	235	TLS	4817.4497	0.1564	175	STELLA	5195.6364	0.6225	348	SOFIN

investigated the presence of a magnetic field during a rotational phase of very good visibility of the spots of overabundant elements.

2 OBSERVATIONS AND DATA REDUCTION

We obtained nine high-quality UVES spectra in 2005 (Hubrig et al. 2006a). We organized a multisite campaign at the end of 2008 and the beginning of 2009 using the Coudé spectrograph of the 2.0-m telescope of the Thüringer Landessternwarte (TLS) (2008 October–2009 February) and the Stella Echelle Spectrograph (SES) spectrograph of the 1.2-m STELLA-I robotic telescope at the Teide Observatory (2008 November–December). The SES spectra have a resolving power of 55 000 and a wavelength coverage of 3880–8820 Å in a fixed spectral format. The exposure time was always 60 min. The spectra were reduced using the SES reduction pipeline (Weber et al. 2008). The spectra obtained with the TLS Coudé spectrograph have a resolving power of ∼67 000 and cover the wavelength region from 3880 to 5470 Å. AR Aur was observed with this instrument twice per night with an exposure time of 30 min. The reduction was carried out with MIDAS procedures. Additionally, we had at our disposal a series of spectroscopic observations obtained from 2002 August to 2003 January with the 2.56-m Nordic Optical Telescope on La Palma using the SOviet-FINnish (SOFIN) échelle spectrograph. Unfortunately, these observations do not have adequate phase coverage and were used only for comparison of line profiles. The SOFIN spectra were reduced with the dedicated software package developed by Ilyin (2000). Since disentangling of the spectra is much more difficult in the phases very close to eclipses, only observations obtained outside of eclipses were selected for the reconstruction of the element distribution. The spectropolarimetric observations of AR Aur at the rotation phase 0.622 were obtained with the low-resolution camera of SOFIN ($R \approx 30\,000$) in spectropolarimetric mode on 2009 December 30.

The observing logbook for SOFIN, TLS and STELLA is presented in Table 1, where the first column gives the date of observation and the second column the corresponding phase. The signal-to-noise ratios (S/N values) per resolution element of the spectra in the wavelength region around 4950 Å and the name of the telescope are listed in columns 3 and 4.

3 DISTRIBUTION OF Fe AND Y ABUNDANCES

In the current analysis, we used the improved DI code IA introduced by Freyhammer et al. (2009). This code uses Tikhonov regularization in a way similar to the DI method described by Piskunov (2008) with a grid of $6^\circ \times 6^\circ$. In the DI reconstruction, we search for the minimum of the regularized discrepancy function, which includes the regularization function and the discrepancy function describing the difference between observed and calculated line profiles. All atomic data in our analysis were taken from the VALD data base (Kupka et al. 1999). For the DI reconstruction, we selected the elements Fe and Y with the clean unblended spectral lines Fe II 4923.9 Å and Y II 4900.1 Å, showing distinct variability over the rotation period. The lines Hg II 3983.9 Å, Sr II 4215.5 Å, and Mn II 4292.2 Å used in our first DI reconstruction (Savanov et al. 2009) with UVES spectra (in the following called SET1) are not usable in the series of spectra obtained with the TLS and STELLA telescopes (in the following called SET2), due to the rather high noise level in the respective wavelength regions. The Ti II 4563.8 Å line, the most suitable Ti line for DI, is in a gap between orders in the UVES observations (SET1).

The results of the reconstruction for both sets are presented in Figs 1 and 2, respectively. The adopted stellar parameters, $T_{\rm eff} = 10\,950$ K, $\log g = 4.33$, were those employed by Nordström & Johansen (1994). The inspection of the resulting Fe and Y distribution maps separated by 4 yr shows that Fe is overabundant by up to +1.5 dex and Y is overabundant by up to +3.9 dex in several spots. Solar values for abundances in the units used in Figs 1 and 2 are −4.50 for Fe and −9.79 for Y (Grevesse et al. 2010). The positions and the shape of the spots with the highest Fe overabundance slightly changed from 2005 to 2009, and the level of the Fe overabundance shows a significant increase, especially in the spot located close to the equator at the phases 0.50–0.75 and in the polar spot at the phases 0.75–0.83. In the Y maps, the evolution of overabundance, shape and position of the spots appears much more remarkable, revealing a region of huge overabundance having a shape of a belt, which is broken around phase zero. Intriguingly, in this phase we observe the hemisphere which is permanently facing the secondary. Such a behaviour is likely observed also for Sr in the UVES spectra and was discussed in our previous study

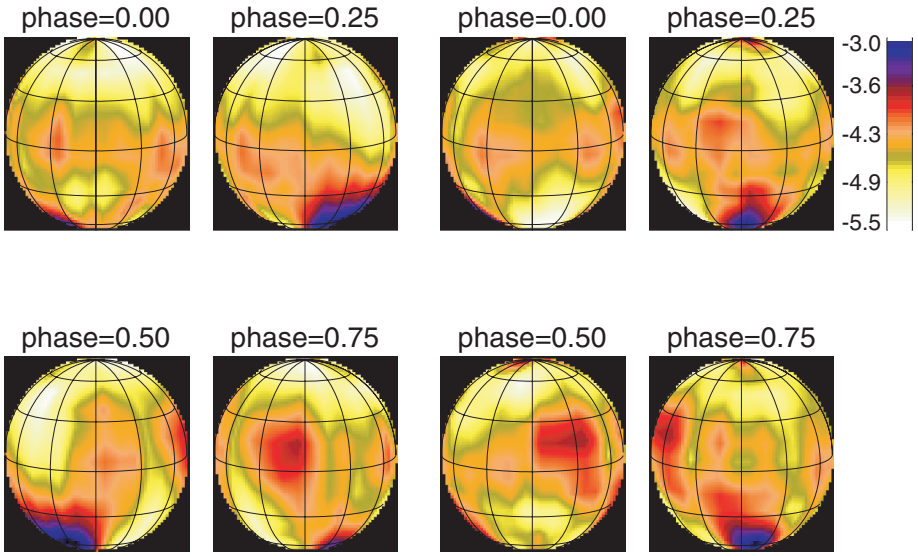

Figure 1. The Fe abundance map of AR Aur obtained from the Fe II 4923.9 Å line for SET1 (left-hand side) and SET2 (right-hand side).

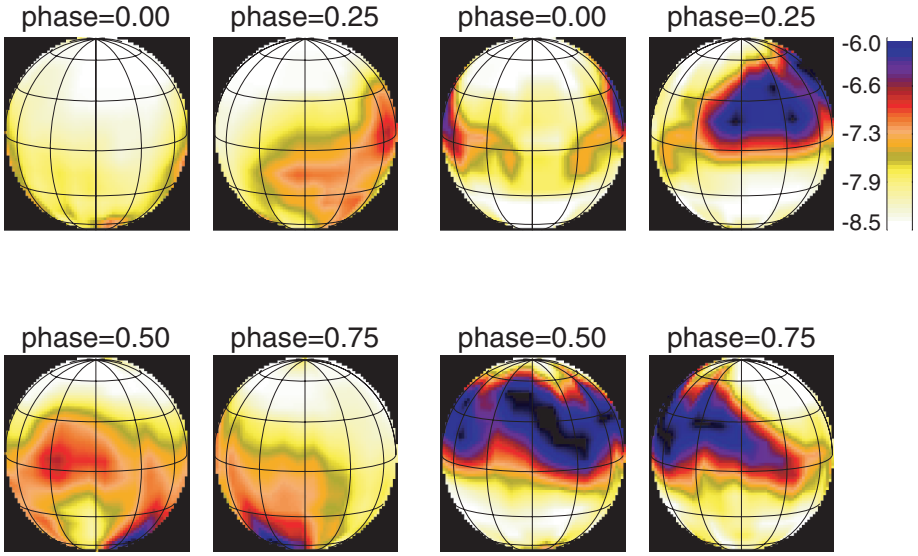

Figure 2. The Y abundance map of AR Aur obtained from the Y II 4900.1 Å line for SET1 (left-hand side) and SET2 (right-hand side).

(Hubrig et al. 2006a). The deviations between the computed and the observed profiles of the order of 0.82–0.85 per cent are nearly equal to the noise of the disentangled spectra.

Our Doppler images were reconstructed with a fixed inclination of the stellar rotational axis of 88°.5, i.e. practically equator-on. Such an inclination causes intrinsic problems for DI because it is not possible to uniquely determine to which hemisphere a spot should be assigned. This 'mirroring effect' is well known in DI and had been documented and simulated in the past for temperature spots (e.g. Piskunov & Wehlau 1994; Rice & Strassmeier 2000). An artefact would be that a spot reconstructed very close to one of the rotational poles could actually stem from the other pole. Therefore, we suggest the reader to be careful when interpreting the spot latitudes.

To confirm the temporal evolution of element inhomogeneities, we made a test involving the SOFIN spectra observed in 2002–2003. Unfortunately, the Y II 4900.1 Å line is lost in the gap between spectral orders and the Fe II 4923.9 Å line is very close to the edge of an order. For this reason, we selected the Sr II 4215.5 Å line, which is strong enough for a comparison with SET1 and SET2. All three sets contain spectra at almost the same rotation phases: 0.81 (SET1), 0.79 (SET2) and 0.79 (SOFIN). Overplotting the line profiles of Sr II 4215.5 Å from this phase indicates that also the Sr spots very likely changed their shape and abundance with time (see Fig. 3).

4 MAGNETIC FIELD DETERMINATION

Since most elements are expected to be inhomogeneously distributed over the surface of the primary of AR Aur, magnetic field measurements were carried out for samples of Ti, Cr, Fe and Y lines separately. The diagnostic potential of high-resolution circularly polarized spectra using the moment technique has been discussed at length in numerous papers by Mathys (e.g. Mathys 1993). Wave-

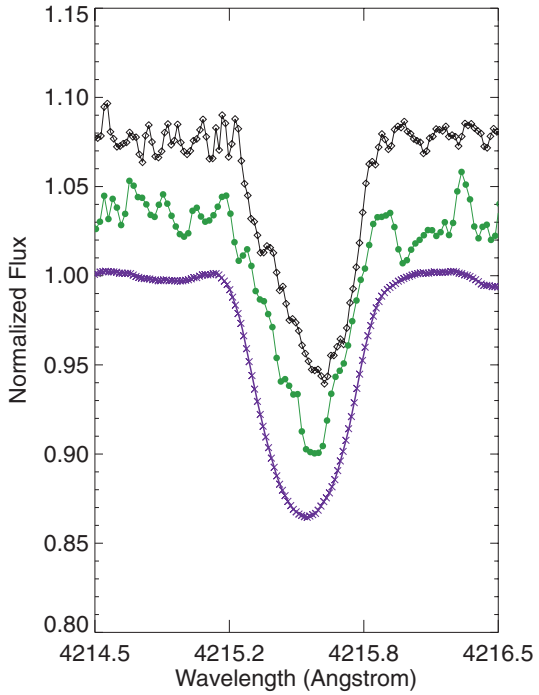

Figure 3. The line profiles of the Sr II 4215.5 Å line at rotation phase ∼0.8 for SET1 (crosses), SET2 (filled circles) and SOFIN spectra (open diamonds). Spectra are shifted in vertical direction for clarity.

Table 2. Magnetic field measurements of AR Aur. *N* is the number of spectral lines used for the measurements.

Element	*N*	$\langle B_z \rangle$ (G)
Primary		
Ti II	9	-519 ± 140
Cr II	8	-454 ± 193
Fe II	16	-372 ± 78
Y II	6	-559 ± 130
Secondary		
Fe II	9	-229 ± 56

length shifts between right- and left-hand side circularly polarized spectra can, in the weak-line approximation, be interpreted in terms of a longitudinal magnetic field $\langle B_z \rangle$. Among the elements showing line variability, the selected elements have numerous transitions in the observed optical spectral region, allowing us to sort out the best samples of clean unblended spectral lines with different Landé factors. The results of our magnetic field measurements, using the formalism described by Mathys (1994), are presented in Table 2, where we indicate the element and the number of measured lines in the first and second columns and the measured longitudinal magnetic field in column 3. A longitudinal magnetic field at a level higher than 3σ of the order of a few hundred gauss is detected in Fe II, Ti II and Y II lines, while a quadratic magnetic field $\langle B \rangle = 8284 \pm 1501$ G at 5.5σ level was measured in Ti II lines. No crossover at 3σ confidence level was detected for the elements studied. Further, we detect a weak longitudinal magnetic field, $\langle B_z \rangle = -229 \pm 56$ G,

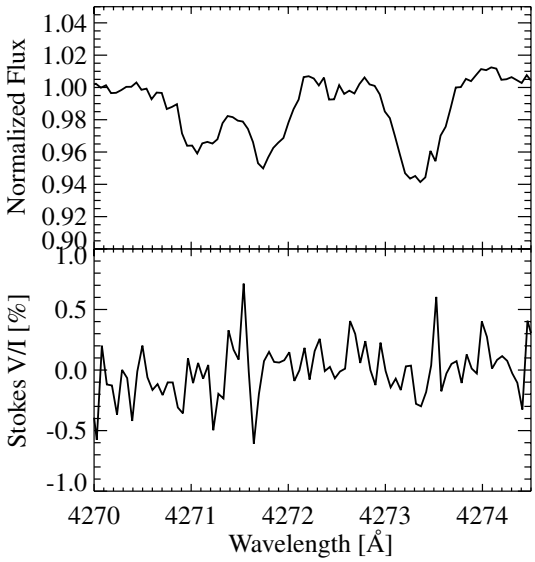

Figure 4. Circular polarization features in the Fe I 4271.8 Å and Fe II 4273.3 Å lines.

in the secondary component using a sample of nine Fe II lines. The main limitation on the accuracy achieved in our determinations is set by the small number of lines that can be used for magnetic field measurements. The diagnosis of the quadratic field is more difficult than that of the longitudinal magnetic field, and it depends much more critically on the number of lines that can be employed. An example of circular polarization signatures is presented in Fig. 4.

The only longitudinal magnetic field measurements carried out for AR Aur were reported recently by Folsom et al. (2010), who used the Least-Square Deconvolution (LSD) technique to combine 1168 lines of various elements. No magnetic field was detected in their analysis of polarimetric spectra obtained in 2006. One possibility for this non-detection could be related to an unfavourable element spot configuration or even to the absence of some element spots at the epoch of their observations, since the authors report that no variability of the Ti and Fe lines was detected. In Fig. 5 we present the distribution of Ti, Fe and Y at the phase 0.622 of the element distribution for SET2. This set was obtained at a time closest to our spectropolarimetric observation and, obviously, spots of higher Fe, Ti and Y concentration are well visible at this phase. On the other hand, very strong Fe and Y element concentrations are almost missing in our first map based on SET1 observations in 2005, which are the closest in time to the spectropolarimetric observations reported by Folsom et al. (2010). We note also that the phase around 0.75, where a spot of enhanced Fe is well visible in our SET1, is completely missing in their observations.

5 DISCUSSION

From a survey of HgMn stars in close spectroscopic binaries, Hubrig & Mathys (1995) suggested that in HgMn stars Hg is probably concentrated along the stellar equator. Until now, DI has been carried out only for α And (e.g. Adelman et al. 2002) and for HD 11753 (Briquet et al. 2010). Kochukhov et al. (2007) discovered secular changes of the mercury distribution in the atmosphere of α And and Briquet et al. (2010) reported evidence for dynamical evolution of several element spots in HD 11753. Including AR Aur, the whole sample of HgMn stars studied with DI consists now of only three HgMn stars. The situation with magnetic field studies is also

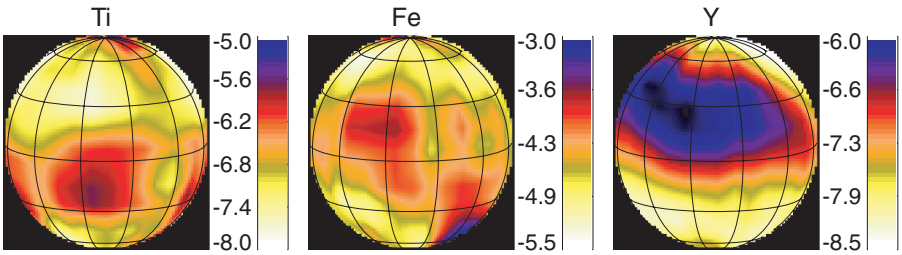

Figure 5. The element distribution from the Ti II 4563.8 Å line, the Fe II 4923.9 Å line and the Y II 4900.1 Å line at the time of our magnetic field measurement (phase 0.622).

very unfortunate, as previous studies never considered to combine element surface mapping with magnetic field measurements. Interestingly, in analogy to the presented detection of a kG quadratic magnetic field in the primary and a weak longitudinal magnetic field in the primary and the secondary of AR Aur, Mathys & Hubrig (1995) reported the detection of a weak magnetic field in the secondary of another SB2 binary, χ Lup, while in the same work they discovered a quadratic magnetic field of 3.6 kG in the primary component of 74 Aqr. The secondaries in both, the AR Aur and χ Lup, systems are mentioned in the literature to have characteristics very similar to early Am stars. Although observational evidence for the presence of magnetic fields in HgMn stars is indeed accumulating, a dedicated survey of magnetic fields for this type of stars is still missing. A previous survey of magnetic fields in 17 HgMn stars (Hubrig et al. 2006b) led to field detections in only four stars. A search for magnetic intensification in a dozen of HgMn stars (Hubrig, Castelli & Wahlgren 1999; Hubrig & Castelli 2001) resulted in the possible presence of a magnetic field only in a few stars. Our study confirms that HgMn stars remain intriguing targets with respect to their temporally evolving anomalies and puzzling topology of magnetic fields. The results achieved in a few individual studies do not allow yet to evaluate theoretical models of the origin of chemical anomalies and their connection with the magnetic field geometry on the stellar surface. Clearly, future element distribution reconstructions using the DI technique and magnetic field measurements using lines of elements concentrated in spots for a larger number of stars are necessary to improve our understanding of physical processes occurring in late B-type binary systems with HgMn primaries.

ACKNOWLEDGMENT

We are grateful to the Deutsche Forschungsgemeinschaft (DFG) for financial support, for SH and IS under DFG grant HU532/13-1, for AT under DFG grant LE1102/2-1, and for MH under DFG grant HA3479/3-3. We would like to thank the anonymous referee for his valuable comments.

REFERENCES

Adelman S. J., Gulliver A. F., Kochukhov O. P., Ryabchikova T. A., 2002, ApJ, 575, 449
Briquet M., Korhonen H., González J. F., Hubrig S., Hackman T., 2010, A&A, 511, A71
Castelli F., Hubrig S., 2004, A&A, 425, 263
Folsom C. P., Kochukhov O., Wade G. A., Silvester J., Bagnulo S., 2010, MNRAS, in press (arXiv:1005.3793)
Freyhammer L. M., Kurtz D. W., Elkin V. G., Mathys G., Savanov I., Zima W., Shibahashi H., Sekiguchi K., 2009, MNRAS, 396, 325
González J. F., Levato H., 2006, A&A, 448, 283
Grevesse N., Asplund M., Sauval A. J., Scott P., 2010, Ap&SS, 328, 179
Hubrig S., Castelli F., 2001, A&A, 375, 963
Hubrig S., Mathys G., 1995, Comments Astrophys., 18, 167
Hubrig S., Castelli F., Wahlgren G. M., 1999, A&A, 346, 139
Hubrig S., González J. F., Savanov I., Schöller M., Ageorges N., Cowley C. R., Wolff B., 2006a, MNRAS, 371, 1953
Hubrig S., North P., Schöller M., Mathys G., 2006b, Astron. Nachrichten, 327, 289
Ilyin I., 2000, PhD thesis, Univ. Oulu
Kochukhov O., Adelman S. J., Gulliver A. F., Piskunov N., 2007, Nat. Phys., 3, 526
Kupka F., Piskunov N., Ryabchikova T. A., Stempels H. C., Weiss W. W., 1999, A&AS, 138, 119
Mathys G., 1993, in Dworetsky M. M., Castelli F., Faraggiana R., eds, Proc. IAU Colloq. 138, ASP Conf. Ser. Vol. 44, Peculiar versus Normal Phenomena in A-type and Related Stars. Astron. Soc. Pac., San Francisco, p. 232
Mathys G., 1994, A&AS, 108, 547
Mathys G., Hubrig S., 1995, A&A, 293, 810
Nordström B., Johansen K. T., 1994, A&A, 282, 787
Piskunov N., 2008, Phys. Scr. 133, 14017
Piskunov N. E., Wehlau W. H., 1994, A&A, 289, 868
Rice J. B., Strassmeier K. G., 2000, A&AS, 147, 151
Savanov I. S., Hubrig S., González J. F., Schöller M., 2009, in Strassmeier K. G., Kosovichev A. G., Backman J. E., eds, Proc. IAU Symp. 259, Cosmic Magnetic Fields: from Planets to Stars and Galaxies. Cambridge Univ. Press, Cambridge, p. 401
Takeda Y., Takada M., Kitamura M., 1979, PASJ, 31, 821
Weber M., Granzer T., Strassmeier K. G., Woche M., 2008, in Bridger A., Radziwill N. M., eds, Proc. SPIE, Vol. 7019, Advanced Software and Control for Astronomy II. Astron. Soc. Pac., San Francisco, p. 19

This paper has been typeset from a TEX/LATEX file prepared by the author.